

TRANSITIONS BETWEEN SUPPRESSED AND ENHANCED DRYING MODES IN PHASE-SEPARATING COATINGS

M. Yamamura, T. Nasu, S. Harada, Y. Mawatari and H. Kage

Department of Applied Chemistry
Kyushu Institute of Technology, Kitakyushu, Fukuoka, Japan 804-8550

Presented at the 16th International Coating Science and Technology Symposium,
September 9-12, 2012, Midtown Atlanta, GA¹

Introduction

Self-organized patterns emerge in polymeric solutions when solvent evaporation quenches the fluids in a particular location in two-phase regions. The drying-induced phase separation, in turn, alters the local distribution of residual solvents. Indeed, classical diffusion theory showed that a common solvent can self-assemble at phase interfaces to minimize the total free energy of mixing, giving rise to a particular core-shell configuration with solvent-rich layers (solvent shells) around polymer-rich phases. In a particular case when neighboring polymer domains coalesce into each other to give interconnected solvent shells, multiple diffusion paths of solvent evolve along the phase interfaces, and guide the solvent diffusion toward the free surface, leading to enhanced solvent drying [1-3] via phase separation. On the other hand, the solvent drying is suppressed [4-6] when solvent molecules are trapped at discontinuous domain interfaces. Despite the recognition that phase structures determine the device performances of photovoltaic [7], and optical coatings, the detailed physical mechanism of enhanced or suppressed solvent evaporation is still an ongoing debate. In this article, we provide the first experimental evidence that the domain growth rate determines the transition between enhanced and suppressed drying modes.

Experimental

Ternary solutions were prepared from different pairs of poly-dimethyl siloxane (PDMS, Aldrich), cellulose acetate (CA, Mn=30,000, Aldrich), cellulose acetate butyrate (CAB, Mn=30,000, Wako), or polystyrene (PS, Mn=115,000, Hayashi) dissolved in methyl ethyl ketone (MEK) or isopropyl acetate (IA) as a common solvent. We used different functionally terminated PDMSs of dihydroxyl-terminated (h-PDMS), diaminopropyl-terminated (a-PDMS), and monoglycidyl-ether-terminated (mg-PDMS). The prepared solution with an initial polymer concentration of 4.76 wt%, was deposited on a glass substrate with an initial film thickness of 400 microns. The coated area was specified to be 36 cm² by gluing a 0.4 mm thick aluminum shim on the substrate. First, the glass surface was cleaned using a plasma etching device (Meiwafosis, SEDE-GE) for 15 min in vacuum before deposition. Then, the substrate was continuously heated by a glass conductive heater (Kitazato MP-10DMH) set beneath the substrate with an air clearance of 0.25 mm. The base temperature of the substrate was maintained by regulating the current through the heater. The coating was then mounted on an electronic balance (Sartorius LP1200S) to measure the decrease in film mass, which was stored in a

¹ Unpublished. ISCST shall not be responsible for statements or opinions contained in papers or printed in its publications.

personal computer at a sampling rate of 2.5 Hz. The solvent drying rate was calculated from each slope of the weight-loss curves as $r = - (1/A)dW/dt$, where A is the film surface area, t the time and W the mass of the film during drying. The residual solvent contents were quantified using the solvent-to-solute mass ratio (u). UV transmittance spectroscopy measurements were carried out for solutions at different solvent concentrations to determine the cloud points, at which the solution enters the thermodynamically unstable two-phase region. The static surface tensions of the solutions were measured using the Wilhelmy plate method to quantify the adsorption behavior of the polymeric components.

Results and Discussion

Figure 1 illustrates a comparison of mass loss curves between ternary and binary polymer solution coatings. The ternary solution was prepared from a-PDMS/CAB blend with mass ratio of 1:4 (wt/wt). The mass loss curve of the ternary solution shows a distinct deviation from that of the binary solution below a particular residual solvent content $u \sim 3$, and indicates a faster solvent drying, i.e., an enhanced drying, in the polymer blend.

The phase morphology of the dried film, corresponding to the case in Fig. 1, indicates that phase structures are interconnected (Fig. 2a and 2b) with a certain gradient in size in the thickness direction (Fig. 2d). The self-organized pattern was highly-ordered and involved a characteristic domain size, as indicated by an isotropic ring pattern in the background-corrected 2D fast Fourier transforms (FFT) images (Fig. 2c).

In order to quantify the enhanced solvent evaporation, we calculated the averaged drying rates of polymer blends at the solvent-to-solute mass ratio of $u_c = 3 \pm 0.5$. Fig. 3 illustrates the dimensionless drying rates for 14 different pairs of polymers i and j with the mass blend ratio of $i / j = 0.1$ (wt/wt), normalized by those in the binary solution of major polymer component j . The dihydroxyl-terminated PDMS (h-PDMS)/CAB system shows the normalized drying rate of 0.48, indicating 48 % increase in solvent drying rates within a certain range of polymer concentrations. However, the remarkable drying enhancement in phase-separating coatings diminished as changing the PDMS chain end group: the normalized drying rate for diaminopropyl-terminated PDMS was 0.21, whereas that for monoglycidyl-ether-terminated PDMS was -0.08, indicating a particular transition from the enhanced to suppressed drying mode.

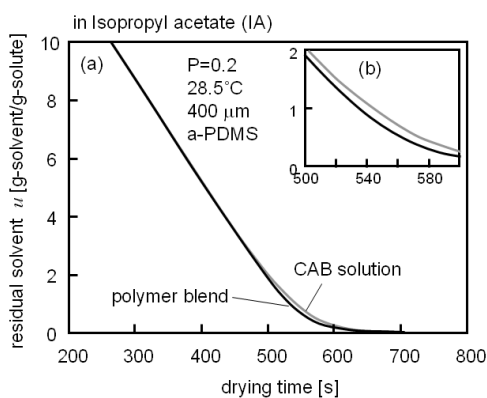


Fig.1 Mass loss curves

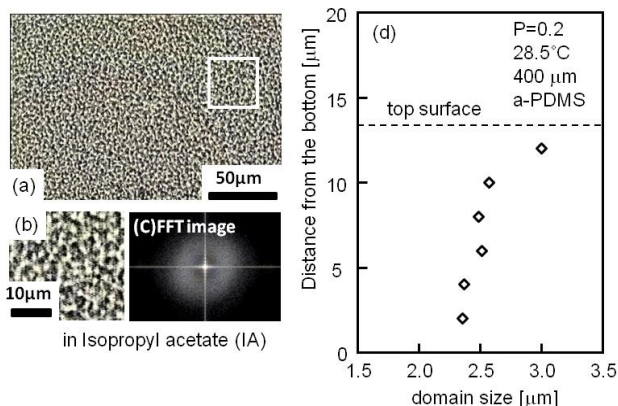


Fig. 2 Microstructures of dried film

To elucidate the drying transition in detail, the mass loss measurements were performed for different blend ratios, drying temperatures, and polymer molecular weights. The systematic measurements revealed that the drying rate variations were correlated by the averaged domain growth rate $d/(t_f - t_c)$, where d denotes the final domain size at the film surface, t_f the time until the end of drying, and t_c the time at the cloud point. As shown in Fig. 4, an increase in the domain growth rate results in a transition from the enhanced (regime I) to suppressed (regime III) drying for a wide range of drying conditions. The transient behavior was observed at the intermediate rates of 0.020~0.03 $\mu\text{m/s}$ (regime II). On the contrary, preliminary characterizations on surface activities of polymeric components, the solvent contents at the cloud points, and the final domain size showed that these physical quantities are not a unique physical factor that dominates the transition between the enhanced and suppressed drying modes. These facts provide conclusive evidence that a faster structure formation tends to trap more solvent molecules at the growing domain interfaces, leading to a slower diffusion in the vicinity of free surface. In contrast, the solvent molecules can diffuse along the interfaces, rather than self-assemble there, in the case when the interface formation is sufficiently slow. The resultant interfacial diffusion possibly guides the solvent transports to give an enhanced drying.

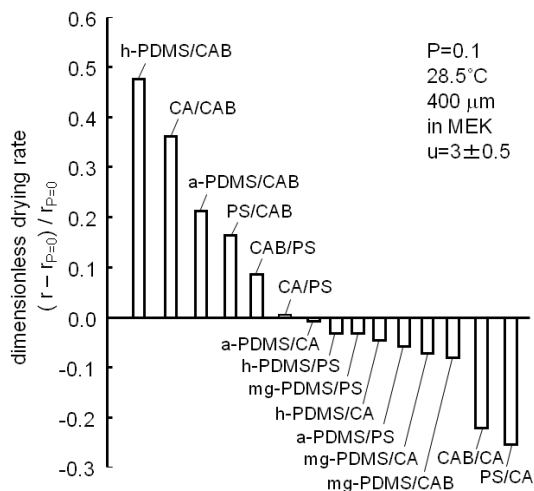


Fig. 3 Drying rate variations in blends (i/j) of polymer component i in j

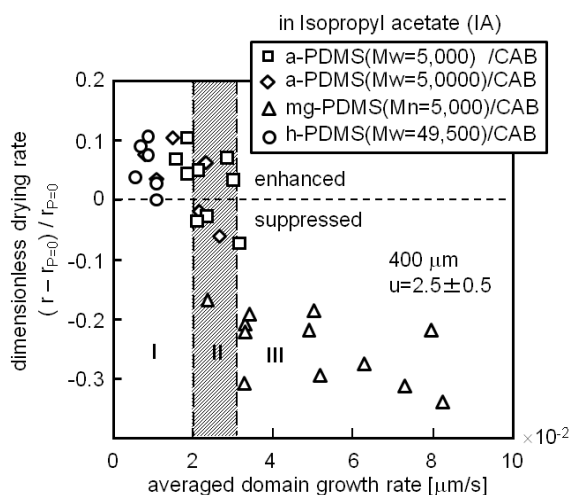


Fig. 4 Transition between enhanced and suppressed drying modes.

References

- [1]M. Yamamura, H. Yoshihara, Y. Mawatari, H. Kage, *Journal of Chemical Engineering of Japan*, 45(2012) 441-443
- [2]M. Yamamura, H. Yoshihara, Y. Mawatari, H. Kage, *Proceeding of the ISCST Symposium* (2008) 114-117
- [3]M. Yamamura, T. Yamakawa, Y. Mawatari, H. Kage, *Proceeding of 9th ECS* (2011) 212-215
- [4]M. Yamamura, K. Horiuchi, T. Kajiwara, K. Adachi, *AIChE Journal* 48 (2002) 2711-2714
- [5]D.M.Vaessen, A.V. McCormick, L.F. Francis, *Polymer*, 43 (2002) 2267-2277
- [6]M. Yamamura, R. Sakomoto, H. Kage, *Proceeding of the ISCST Symposium* (2004) 179-182
- [7]M. Sanyal, B.Schmidt-Hansberg, M.F.G. Klein, C. Munuera, A. Vorobiev, A. Colsmann, P. Scharfer, U. Lemmer, W. Schabel, H. Dosch, E. Barrena, *Macromolecules*, 44 (2011) 3795-3800